

Analysis of Linear Coaxial Antennas

Jean-Fu Kiang, *Member, IEEE*

Abstract— Two types of linear coaxial antennas, coaxial-colinear antennas, and slotted coaxial antennas are studied to check the possibility of using them as the base-station antenna in personal communication systems. The slot voltages and input impedance of linear coaxial antennas are obtained by using a transmission-line analysis where the radiation effect is accounted by a shunt and a serial admittance, respectively. The current distribution is obtained by solving an integral equation using the method of moments. The radiation pattern and directivity are then obtained from the current distribution and the reflection coefficient inside the coaxial cable. Factors analyzed include frequency, coaxial filling permittivity, and segment number.

Index Terms— Coaxial-colinear antenna, field pattern, gain, input impedance, slotted coaxial antenna, transmission line analysis.

I. INTRODUCTION

COAXIAL cables have been widely used to feed signal to microwave antennas or transmit signals from antennas to receivers. The cable openings can also be used as radiators after some modifications. In [1], a coaxial cable opening is flared out to increase its radiation efficiency. The fields in space and inside the coaxial cable are expanded in terms of eigen functions and the fields in the flared region are expanded by using the finite-element method. In [2], a power conservation technique is applied to analyze a coaxial-fed monopole antenna. In [3], a coaxial opening is flushed with an infinitely large ground plane and the center conductor is mounted with a hemisphere to reduce signal reflection.

Coaxial colinear antennas have been considered as array elements to replace two-dimensional dipole arrays because the feeding structure of the former is much simpler than that of the latter [4]–[6]. In [7], a Snyder dipole is analyzed, which is a simplified version of the coaxial-colinear antenna. In this paper, a single coaxial-colinear antenna is considered as a base-station antenna for personal communication systems due to its low cost and structural simplicity. It consists of several segments of half-wavelength coaxial cables where the inner conductor of one cable is electrically connected to the outer conductor of the adjacent one [4]–[6]. The intent is to have the excitation voltages across all the slots in phase and equal in magnitude so that a stronger in-phase current distribution can

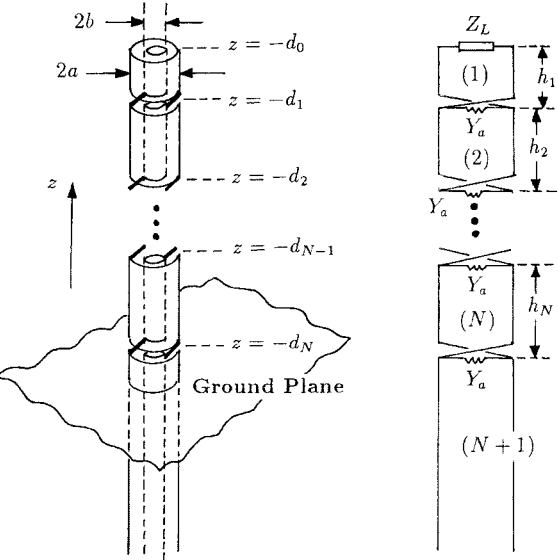


Fig. 1. Configuration of a coaxial-colinear antenna and its equivalent transmission line model.

be driven on the outer surface of the coaxial cable to obtain a high gain in the broadside direction.

Circumferential slots on a cylindrical waveguide surface have been analyzed for its admittance [8]. In [9], a full-wave analysis has been applied to study the radiation properties of a circumferential slot on the outer conductor of a coaxial cable. A slotted coaxial cable also has the potential to achieve slot voltages of equal magnitude and phase if the length of each segment is one wavelength of the dominant mode in the coaxial cable. Such a structure can be made by peeling off the outer conductor at regular intervals, which is simpler than making a coaxial colinear antenna. Since the wavelengths inside and outside the coaxial cable are different, changing the dielectric constant of the coaxial-filling material implies changing the physical length of each segment, which is a half (full) wavelength of the dominant mode inside the coaxial cable for the coaxial-colinear (slotted coaxial) antenna. The location change of multiple excitation sources affects the current distribution on the outer surface of coaxial cable, hence, affects the radiation-field pattern.

The radiation power can be viewed as a power loss from inside the coaxial cable and can be modeled as a shunt or serial admittance across the slot between two adjacent transmission line segments, as shown in Figs. 1 and 2. Thus, the reflection coefficient and input impedance looking from the feeding coaxial cable can be obtained by solving the transmission line

Manuscript received October 18, 1996; revised November 6, 1997. This work was supported by the National Science Council, Taiwan, R.O.C., under Contract NSC-86-2221-E005-021 and the Telecommunication Laboratories, Chunghwa Telecom Co., Ltd., under Contract NSC-86-2209.

The author is with the Department of Electrical Engineering, National Chung-Hsing University, Taichung, Taiwan, R.O.C.

Publisher Item Identifier S 0018-926X(98)03370-5.

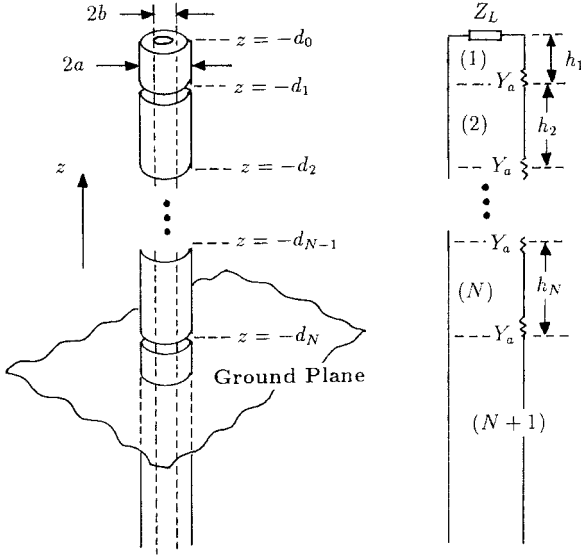


Fig. 2. Configuration of a slotted coaxial antenna and its equivalent transmission line model.

equations. These two parameters are then used to calculate the directivity of the linear coaxial antennas for further analysis, which is an important factor in designing the base-station antenna for personal communication systems.

II. TRANSMISSION LINE ANALYSIS

It is very complicated to solve the antenna problems shown in Figs. 1 and 2 rigorously. One possible solution involves expanding the fields inside the coaxial cable by using a set of coaxial waveguide modes and expanding the fields in the gap regions by using a set of finite elements. The fields outside of the coaxial cable can be expressed in terms of the current on the outer conductor surface and the Green's function. Then the solution is obtained by matching all the tangential fields across all the gaps concurrently.

In this paper, we try to solve the problem in two parts. For waves guided inside the cable, the gaps can be viewed as equivalent admittances that consume the guided power. The admittance of a single slot on an infinitely long cylinder is used in the sense that the power radiated from such a slot is the same as the power loss across an equivalent admittance connected in the transmission line. Then, equivalent transmission lines incorporating these admittances are derived for both antennas as shown in Figs. 1 and 2. The voltage across each admittance solved from the transmission line analysis is taken as the voltage drop across the corresponding gap. These voltage drops are then used to drive the currents on the outer surface of the cable.

In this approach, the interaction among currents on the coaxial outer surface and the interaction among slots inside the coaxial cable are included, but the coupling from the current on the outer surface into the inner surface is not considered. This solution procedure is significantly simpler than the rigorous full-wave solution and its validity will be verified later by comparing with results in the literatures, as shown in Figs. 3–5.

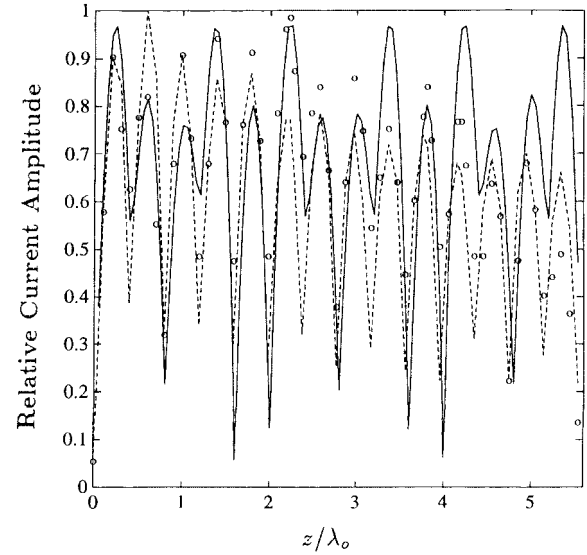


Fig. 3. Current amplitude of an end-fed 14-element coaxial-colinear antenna: $f = 1060$ MHz, $a = 1.4$ mm, $d = 0.2$ mm, $Z_\ell = 167\Omega$, $Z_L = 0$, $\epsilon = 1.6\epsilon_0$. —: this approach; - - -: numerical method in [6]; o: experiment in [6].

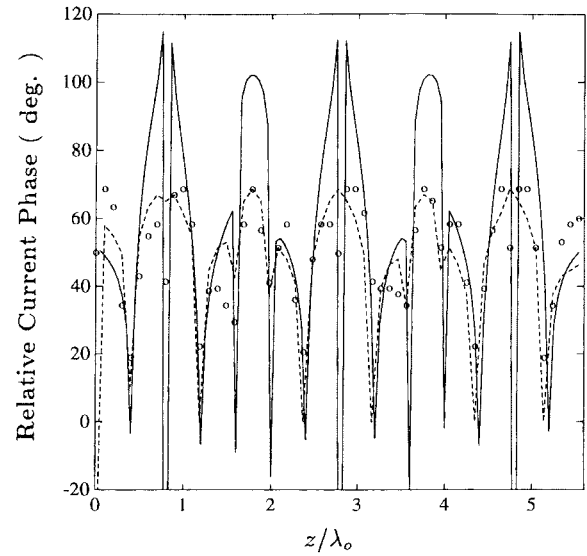


Fig. 4. Current phase of an end-fed 14-element coaxial-colinear antenna; all parameters are the same as in Fig. 3.

For the coaxial-colinear antenna (shown in Fig. 1) the TEM mode inside the waveguide can be modeled by using the transmission line equations [10]. The voltage and current waves in each segment are

$$\begin{aligned} V_\ell(z_\ell) &= V_\ell^+ e^{ik_\ell z_\ell} + V_\ell^- e^{-ik_\ell z_\ell}, \quad 1 \leq \ell \leq N \\ I_\ell(z_\ell) &= \frac{1}{Z_\ell} (V_\ell^+ e^{ik_\ell z_\ell} - V_\ell^- e^{-ik_\ell z_\ell}), \quad 1 \leq \ell \leq N \\ V_{N+1}(z_{N+1}) &= V_o (e^{ik_{N+1} z_{N+1}} + \Gamma e^{-ik_{N+1} z_{N+1}}) \\ I_{N+1}(z_{N+1}) &= \frac{1}{Z_{N+1}} V_o (e^{ik_{N+1} z_{N+1}} - \Gamma e^{-ik_{N+1} z_{N+1}}) \end{aligned} \quad (1)$$

where $z_\ell = z + d_\ell$ for $1 \leq \ell \leq N$, $z_{N+1} = z + d_N$, the length of the ℓ th segment is $h_\ell = d_\ell - d_{\ell-1}$, $Z_\ell = 60 \log(a_\ell/b_\ell)/\sqrt{\epsilon_\ell/\epsilon_0}$ is the characteristic impedance of the

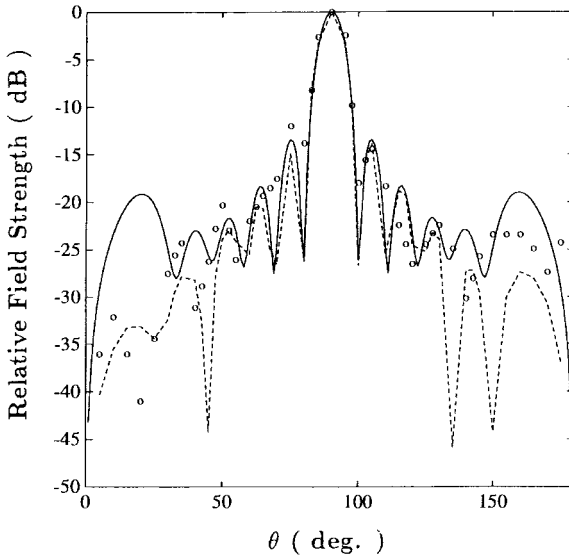


Fig. 5. E -plane field pattern of an end-fed 14-element coaxial-colinear antenna. $f = 1060$ MHz, $a = 1.4$ mm, $d = 0.2$ mm, $Z_\ell = 167\Omega$, $Z_L = 0$, $\epsilon = 1.6\epsilon_0$. —: this approach; - - -: numerical method in [6]; o: experiment in [6].

ℓ th segment with outer radius a_ℓ and inner radius b_ℓ , $k_\ell = \omega\sqrt{\mu\epsilon_\ell}$ is the wave number in segment (ℓ) , V_ℓ^+ and V_ℓ^- are the amplitudes of the voltage waves propagating in the \hat{z} and $-\hat{z}$ direction, respectively. V_o is the amplitude of the incident voltage wave in the feeding coaxial and Γ is the reflection coefficient of the incident voltage wave at the junction $z = -d_N$. Here, the time variation of $e^{-i\omega t}$ is used.

If a load impedance Z_L is attached to the end of the coaxial antenna at $z = -d_0$, we have $V_1(h_1) = Z_L I_1(h_1)$ or

$$V_1^+ e^{ik_1 h_1} + V_1^- e^{-ik_1 h_1} = \frac{Z_L}{Z_1} (V_1^+ e^{ik_1 h_1} - V_1^- e^{-ik_1 h_1}). \quad (2)$$

Z_L is a constant if the load is a resistor, zero (infinity) if the end is short-circuited (open-circuited), or a function of frequency if the load is an inductor or a capacitor.

Due to the transposition of inner and outer conductors at the junction $z = -d_\ell$, the voltage drop across the slot is equal to the voltage at one end of the coaxial cable segment. To satisfy the Kirchhoff's voltage and current laws at the junctions of the equivalent circuit, shown in Fig. 1, we have

$$V_\ell(z_\ell = 0) = -V_{\ell+1}(z_{\ell+1} = h_{\ell+1}), \quad 1 \leq \ell \leq N-1$$

$$\begin{aligned} I_{\ell+1}(z_{\ell+1} = h_{\ell+1}) - Y_a V_{\ell+1}(z_{\ell+1} = h_{\ell+1}) \\ = I_\ell(z_\ell = 0), \quad 1 \leq \ell \leq N-1. \end{aligned} \quad (3)$$

Explicitly,

$$V_\ell^+ + V_\ell^- = -V_{\ell+1}^+ e^{ik_{\ell+1} h_{\ell+1}} - V_{\ell+1}^- e^{-ik_{\ell+1} h_{\ell+1}} \quad 1 \leq \ell \leq N-1$$

$$\begin{aligned} \frac{1}{Z_{\ell+1}} (V_{\ell+1}^+ e^{ik_{\ell+1} h_{\ell+1}} - V_{\ell+1}^- e^{-ik_{\ell+1} h_{\ell+1}}) \\ - Y_a (V_{\ell+1}^+ e^{ik_{\ell+1} h_{\ell+1}} + V_{\ell+1}^- e^{-ik_{\ell+1} h_{\ell+1}}) \\ = -\frac{1}{Z_\ell} (V_\ell^+ - V_\ell^-), \quad 1 \leq \ell \leq N-1. \end{aligned} \quad (4)$$

Similarly, at the junction $z = -d_N$ we have

$$\begin{aligned} V_N^+ + V_N^- &= -V_o(1 + \Gamma) \\ \frac{V_o}{Z_{N+1}} (1 - \Gamma) - Y_a V_o(1 + \Gamma) &= -\frac{1}{Z_N} (V_N^+ - V_N^-). \end{aligned} \quad (5)$$

In (4) and (5), Y_a is the admittance of a circumferential slot on the outer surface of the coaxial cable, which can be calculated as [9], [11]

$$Y_a = \frac{P^*}{|V|^2} = a \int_{-\infty}^{\infty} dk_z \frac{i\omega\epsilon_o}{k_\rho} \text{sinc}^2 \left(\frac{k_z d}{2} \right) \frac{H_1^{(1)}(k_\rho a)}{H_0^{(1)}(k_\rho a)} \quad (6)$$

where a is the outer radius of the coaxial cable, d is the width of the circumferential slot, $k_\rho = \sqrt{k_o^2 - k_z^2}$, P is the radiated power from a slot with a voltage drop V across it. The function $\text{sinc}(x)$ is defined as $\sin(x)/x$. Next, (2), (4), and (5) are solved to obtain the coefficients Γ and V_ℓ^\pm with $1 \leq \ell \leq N$. The voltage drop across the slot at $z = -d_\ell$ is

$$V_{\ell g} = V_\ell^+ + V_\ell^-, \quad 1 \leq \ell \leq N. \quad (7)$$

For the slotted coaxial antennas shown in Fig. 2, the voltage drop across the slot is the voltage difference between the ends of two adjacent segments. Thus, the voltage and current waves at two sides of $z = -d_\ell$ are related by

$$\begin{aligned} Y_a [V_{\ell+1}(z_{\ell+1} = h_{\ell+1}) - V_\ell(z_\ell = 0)] &= I_\ell(z_\ell = 0) \\ 1 \leq \ell &\leq N-1 \end{aligned}$$

$$I_{\ell+1}(z_{\ell+1} = h_{\ell+1}) = I_\ell(z_\ell = 0), \quad 1 \leq \ell \leq N-1. \quad (8)$$

Explicitly,

$$\begin{aligned} V_{\ell+1}^+ e^{ik_{\ell+1} h_{\ell+1}} + V_{\ell+1}^- e^{-ik_{\ell+1} h_{\ell+1}} - (V_\ell^+ + V_\ell^-) \\ = \frac{1}{Y_a Z_\ell} (V_\ell^+ - V_\ell^-), \quad 1 \leq \ell \leq N-1 \\ \frac{1}{Z_{\ell+1}} (V_{\ell+1}^+ e^{ik_{\ell+1} h_{\ell+1}} - V_{\ell+1}^- e^{-ik_{\ell+1} h_{\ell+1}}) \\ = \frac{1}{Z_\ell} (V_\ell^+ - V_\ell^-), \quad 1 \leq \ell \leq N-1. \end{aligned} \quad (9)$$

Similarly, at the junction $z = -d_N$ we have

$$\begin{aligned} V_o(1 + \Gamma) - (V_N^+ + V_N^-) &= \frac{1}{Y_a Z_N} (V_N^+ - V_N^-) \\ \frac{V_o}{Z_{N+1}} (1 - \Gamma) &= \frac{1}{Z_N} (V_N^+ - V_N^-). \end{aligned} \quad (10)$$

Next, (2), (9), and (10) are solved to obtain the coefficients Γ and V_ℓ^\pm with $1 \leq \ell \leq N$. The voltage drop across the slot at $z = -d_\ell$ is

$$\begin{aligned} V_{\ell g} &= (V_\ell^+ + V_\ell^-) - (V_\ell^+ e^{ik_{\ell+1} h_{\ell+1}} + V_\ell^- e^{-ik_{\ell+1} h_{\ell+1}}) \\ 1 \leq \ell &\leq N. \end{aligned} \quad (11)$$

III. CURRENT DISTRIBUTION AND RADIATION FIELD

The electric field $\bar{E}(\bar{r})$ generated by the current on the outer surface of a wire antenna $\bar{J}(\bar{r})$ can be expressed as [12]

$$\begin{aligned} \bar{E}(\bar{r}) = i\omega\mu \int_S d\bar{r}' \frac{\bar{J}(\bar{r}') e^{ik_0|\bar{r}-\bar{r}'|}}{4\pi|\bar{r}-\bar{r}'|} - \frac{1}{i\omega\epsilon_0} \nabla \\ \cdot \int_S d\bar{r}' \frac{\nabla' \cdot \bar{J}(\bar{r}') e^{ik_0|\bar{r}-\bar{r}'|}}{4\pi|\bar{r}-\bar{r}'|}. \end{aligned} \quad (12)$$

Once the voltage drop across the slots are obtained, the current distribution on the outer surface of the coaxial cable can be obtained by solving the integral equation using the method of moments [12]

$$\bar{E}(\bar{r}) = \begin{cases} -\hat{z}V_\ell\delta(\bar{r}-\bar{r}_\ell), & \text{on the } \ell\text{th slot} \\ 0, & \text{elsewhere} \end{cases} \quad (13)$$

where V_ℓ is the voltage drop across the ℓ th slot at \bar{r}_ℓ . A set of one-dimensional linear basis functions are chosen to expand the surface current, then another set of step functions are chosen as the weighting functions.

Assume that an infinite ground plane is placed at half of a segment length below the N th slot, then the image method can be used to replace the original problem by an equivalent cable radiating in free-space [11]. The equivalent cable has twice the length of the original cable above the ground plane and has twice the number of excitation slots. The amplitude of the excitation voltage across each slot is the same as that of its image.

The radiation field pattern can be calculated from (12) once the current distribution is solved from (13). The directivity D of the antenna is defined as the maximum power density over the power density of an isotropic radiator which radiates the same amount of power as the original radiator. Thus, we have

$$D = \frac{|\bar{E}|_{\max}^2 / \eta_0}{|V_0|^2 (1 - |\Gamma|^2) / (Z_{N+1} 4\pi r^2)} \quad (14)$$

where $\eta_0 = \sqrt{\mu/\epsilon_0}$ is the intrinsic impedance of free-space, r is the distance from the observation point to the origin, and $|\bar{E}|_{\max}$ is the maximum electric field strength in all directions.

IV. NUMERICAL RESULTS AND DISCUSSIONS

In Figs. 3 and 4, the current distributions on the outer surface of a 14-element end-fed coaxial–colinear antenna are shown. The amplitude obtained by this approach match reasonably well with the experimental result in [6]. The discrepancy is more obvious away from the feeding cable end because this approach assumes no conductor or dielectric loss, while the numerical results in [6] assume an attenuation constant for the TEM mode propagating inside each cable segment. The phase variation obtained by this approach is more rapid near some slot locations.

The comparison shows that our approach is correct. If the dielectric and conductor losses inside the coaxial cable are considered, the gap voltages are expected to decrease in the propagation direction of the TEM mode. In such circumstances, the gap voltages can still be obtained by

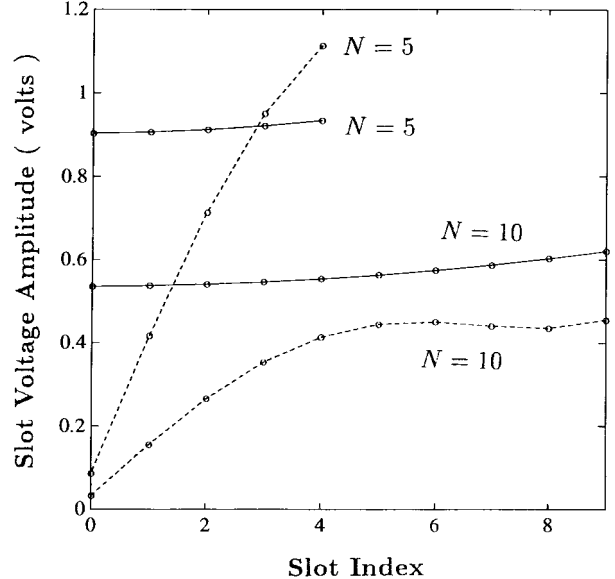


Fig. 6. Slot voltage amplitude of linear coaxial antennas. —○—: coaxial–colinear antenna, $f = 995$ MHz, $a = 1.2$ cm, $b = 0.4$ cm, $d = 0.2$ cm, $\epsilon = 3.75$ cm, $h = 7.5$ cm, $Z_L = 0$, $\epsilon = 4\epsilon_0$. -○-: slotted coaxial antenna, parameters are the same as the coaxial–colinear antenna except that $h = 15$ cm.

using the transmission line analysis in our approach without assuming any attenuation constant of the TEM mode.

Fig. 5 shows the field pattern in the E plane and our results match well with both the numerical and experimental data in [6] around the main beam pointing in the xy plane. In the $-\hat{z}$ direction, our results are closer to the measurement data than the numerical data in [6] are and vice versa in the \hat{z} direction.

Fig. 6 shows the slot-voltage amplitude of both a coaxial–colinear and a slotted coaxial antenna. The amplitude of the incident voltage wave is one volt. The abscissa indicates the slot order instead of a real distance. Since the intent is to have the slot voltage equal in phase and magnitude as discussed in the introduction, the segment length of the slotted coaxial antenna is twice that of the coaxial colinear antenna with the same filling permittivity. Thus, the total length of the slotted coaxial antenna is roughly twice that of the coaxial–colinear antenna with the same number of slots. In Fig. 6, the slot voltage is quite uniform for a coaxial–colinear antenna, but a significant tapering is observed for the slotted coaxial antenna. The associated phase variation of both antennas are shown in Fig. 7. The phases of all the slot voltages in a coaxial–colinear antenna are quite uniform and a smooth phase variation is observed for the slotted coaxial antenna.

The input impedance looking from the feeding coaxial segment $N + 1$ is related to the reflection coefficient Γ by

$$Z_{in} = \frac{\eta_{N+1}}{2\pi} \log \left(\frac{a_{N+1}}{b_{N+1}} \right) \frac{1 + \Gamma}{1 - \Gamma} \quad (15)$$

where $\eta_{N+1} = \sqrt{\mu/\epsilon_{N+1}}$ is the intrinsic impedance of the TEM mode in coaxial segment $N + 1$. The reflection coefficients incurred by a single circumferential slot on the outer surface of an infinitely long coaxial cable are shown in Fig. 8. In the low frequencies, the reflection coefficient obtained by the transmission line analysis is about 10%

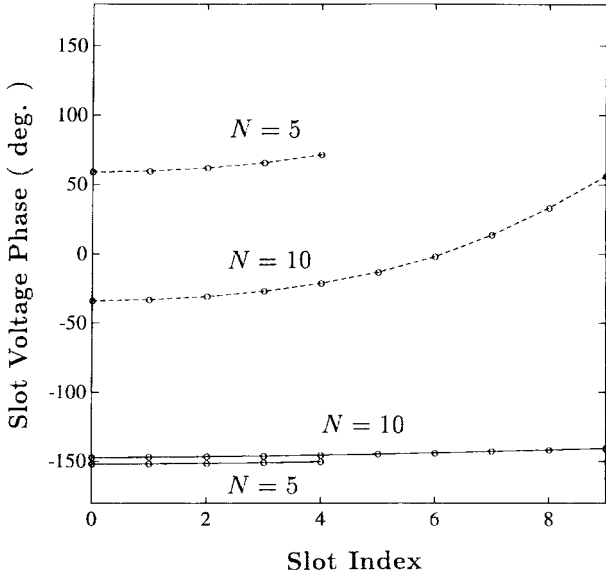


Fig. 7. Slot-voltage phase; parameters are the same as in Fig. 6.

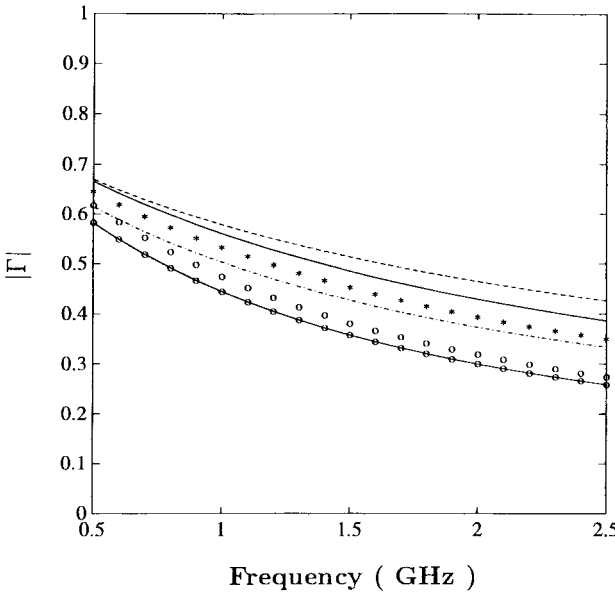


Fig. 8. Magnitude of reflection coefficient caused by a circumferential slot in an infinitely long coaxial cable, $a = 1.2$ cm, $b = 0.4$ cm. —: transmission line analysis (TLA), $d = 0.1$ cm, $\epsilon = 1.5\epsilon_0$; - - -: TLA, $d = 0.3$ cm, $\epsilon = 1.5\epsilon_0$; - - - -: TLA, $d = 0.1$ cm, $\epsilon = \epsilon_0$; o: full-wave analysis (FWA), $d = 0.1$ cm, $\epsilon = 1.5\epsilon_0$; *: FWA, $d = 0.3$ cm, $\epsilon = 1.5\epsilon_0$; —o—: FWA, $d = 0.1$ cm, $\epsilon = \epsilon_0$.

different from that of the full-wave analysis in [9] where all the higher order modes in the cable are considered.

Fig. 9 shows the input impedance of a coaxial-colinear antenna. The variation range is small over a 10% bandwidth centered at 1 GHz. The input impedance of the counterpart slotted coaxial antenna is shown in Fig. 10. The frequency dependence shows a resonance behavior near 980 MHz when $N = 5$ and near 995 MHz when $N = 10$. This implies that the coaxial-colinear antenna has a wider bandwidth than that of the slotted coaxial antenna in the sense of input impedance.

The field patterns in the E -plane are shown in Fig. 11. The number of sidelobes for the coaxial-colinear antenna increases

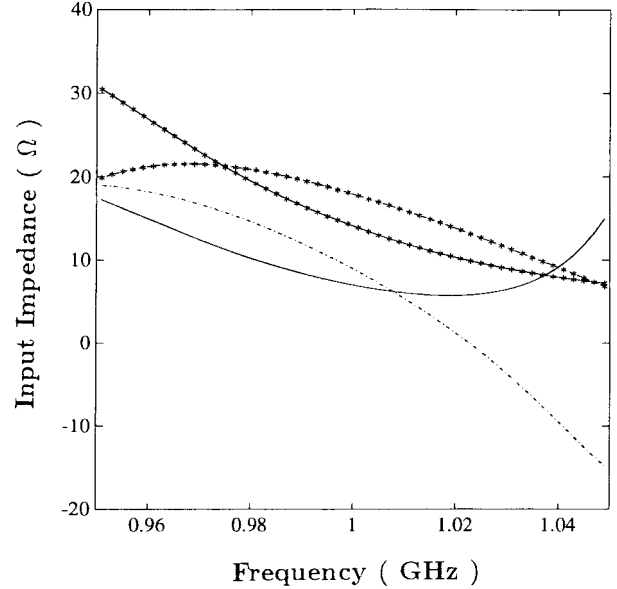


Fig. 9. Frequency variation of the input impedance of a coaxial-colinear antenna, $a = 1.2$ cm, $b = 0.4$ cm, $d = 0.2$ cm, $e = 3.75$ cm, $h = 7.5$ cm, $Z_L = 0$, $\epsilon = 4\epsilon_0$. —: real part for $N = 10$; - - -: imaginary part for $N = 10$, *—: real part for $N = 5$; - - - -: imaginary part for $N = 5$.

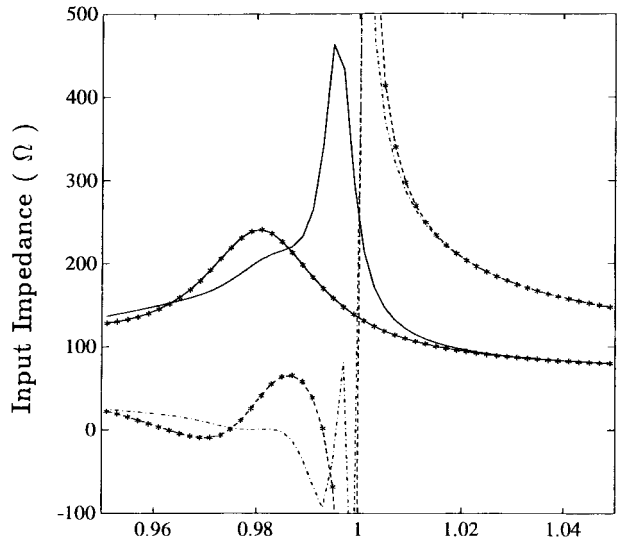


Fig. 10. Frequency variation of the input impedance of a slotted coaxial antenna; parameters are the same as in Fig. 9 except that $h = 15$ cm.

from two with $N = 5$ to four with $N = 10$, while the number of sidelobes for the slotted coaxial antenna increases from three with $N = 5$ to four with $N = 10$. Most of the sidelobe magnitude of the coaxial-colinear antenna is higher than that of the counterpart slotted coaxial antenna by 10–25 dB, except that the first slotted coaxial sidelobe is higher than the first coaxial-colinear sidelobe with $N = 10$. As the segment number increases, the sidelobe level of both antennas decreases.

For reflector antennas like paraboloid dishes, tapering the illuminating field reduces the amplitude of sidelobes, but usually at the price of increasing the main beamwidth. If we make an analog between the slot-voltage distribution along the cable with the field distribution on the reflector dish, the

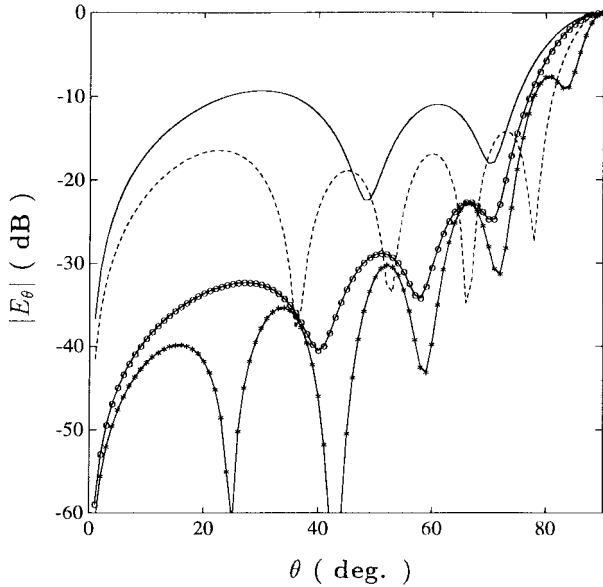


Fig. 11. E -plane field pattern of linear coaxial antennas, $f = 995$ MHz, $a = 1.2$ cm, $b = 0.4$ cm, $d = 0.2$ cm, $e = 3.75$ cm, $h = 7.5$ cm for coaxial-colinear antenna (CCA), $h = 15$ cm for slotted coaxial antenna (SCA), $Z_L = 0$, $\epsilon = 4\epsilon_0$. —: $N = 5$ for CCA; - - -: $N = 10$ for CCA; - - o - : $N = 5$ for SCA; - * - : $N = 10$ for SCA.

slotted coaxial antenna has a tapering slot-voltage distribution, hence, the sidelobes level is reduced. It is interesting to notice that the main beamwidth is also narrower than that of a coaxial-colinear antenna. However, the physical length of the slotted coaxial antenna is about twice that of the coaxial-colinear antenna and the current distribution (which is the real radiating source) on the coaxial outer surface is not quite smooth as indicated in Fig. 3.

To be considered as a base-station antenna in personal communication systems, directivity or antenna gain in the horizontal plane is an important factor. In Fig. 12, we show the directivity of both types of antennas. The directivity of coaxial-colinear antennas are relatively insensitive to frequency and is higher than that of the counterpart slotted coaxial antennas. On the other hand, the directivity of the slotted coaxial antennas are more sensitive to frequency. This implies that the bandwidth of the slotted coaxial antenna is narrower than that of the coaxial-colinear antenna in the sense of directivity.

Over most of the frequencies considered, the main beam points in the horizontal direction ($\theta = 90^\circ$). For the coaxial-colinear antenna with $N = 10$, the maximum field direction switches away from the horizon when $f > 1,043$ MHz. For the slotted coaxial antenna with $N = 5$ ($N = 10$), the maximum field direction switches away from the horizon when $f \leq 965$ MHz ($f \leq 992$ MHz). These frequency ranges are associated with the abrupt changes of directivity in Fig. 12.

Since the permittivity of the coaxial cable filling determines the segment length and the slot locations, which, in turn, determines the current distribution and the field pattern, we calculate the directivity of both types of antennas with different filling permittivity and the results are shown in Fig. 13. As the permittivity is changed from ϵ_0 to $6\epsilon_0$, the directivity of

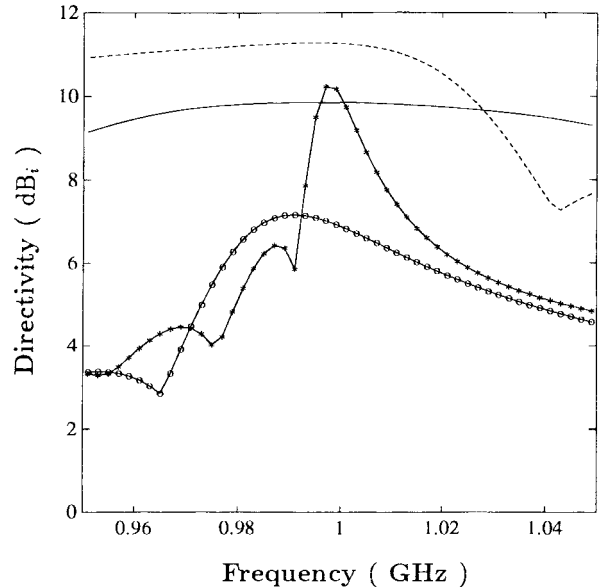


Fig. 12. Frequency dependence of directivity of linear coaxial antennas; all parameters other than frequency are the same as in Fig. 11.

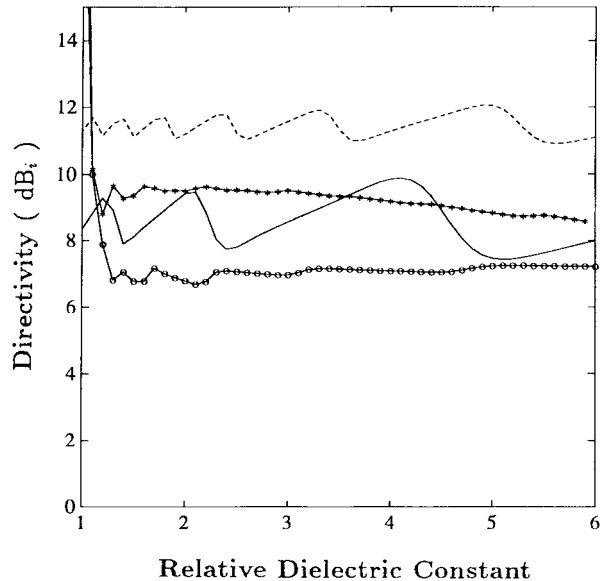


Fig. 13. Effects of coaxial filling permittivity on the directivity of linear coaxial antennas; all parameters other than ϵ are the same as in Fig. 11.

the coaxial-colinear antenna varies up and down around a constant which is 8.5 dB_i when $N = 5$ and is 11.5 dB_i when $N = 10$. The directivity of slotted coaxial antenna shows slight variation, the high directivity at low permittivity occurs where the main beam points far away from the horizon. For $N = 5$, the maximum field angle is 17° , 27° , and 21° when ϵ equals ϵ_0 , $1.1\epsilon_0$, and $1.2\epsilon_0$, respectively. For $N = 10$, the maximum field angle is 12° , 12° , and 13° when ϵ equals ϵ_0 , $1.1\epsilon_0$, and $1.2\epsilon_0$, respectively.

Finally, the effects of segment number on the directivity are calculated and shown in Fig. 14. For the coaxial-colinear antenna, the directivity shows an alternative high-low pattern when the segment number is increased. The alternation magnitude becomes smaller with increasing N and the directivity

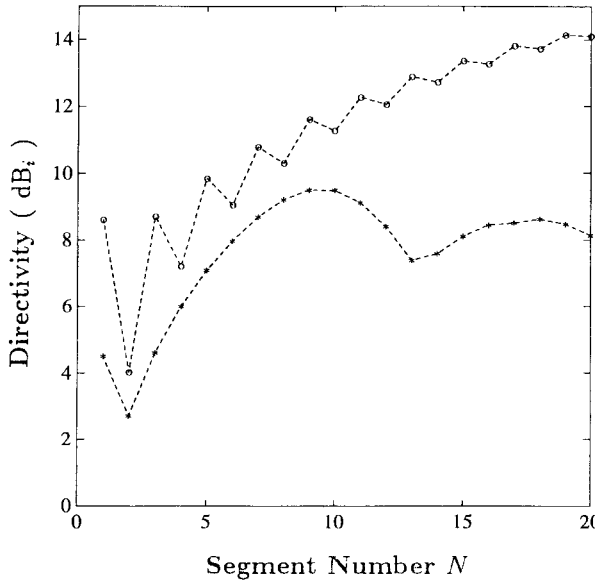


Fig. 14. Effects of coaxial segment number on the directivity of linear coaxial antennas; all parameters other than N are the same as in Fig. 11. -o--: coaxial colinear antenna; -*--: slotted coaxial antenna.

reaches a saturation value of 14.2 dB_i around $N = 19$. The directivity of the slotted coaxial antenna reaches a maximum of 9.5 dB_i around $N = 10$ and decreases when the segment number is further increased.

The physical length of the slotted coaxial antenna is about twice that of the coaxial–colinear antenna with the same number of segments. This should also be considered in designing the base-station antenna for personal communication systems.

V. CONCLUSIONS

A transmission line analysis incorporating the radiation effects has been developed to analyze and compare the coaxial–colinear and slotted coaxial antennas for possible use as base-station antennas for personal communication systems. The slot voltage, current distribution, input impedance, field pattern, and directivity are calculated to study the effects of frequency, cable filling permittivity, and segment number. The coaxial–colinear antenna has a wider bandwidth than its counterpart slotted coaxial antenna in the sense of input impedance and directivity. The directivity of the coaxial colinear antenna is higher than that of the counterpart slotted coaxial antenna and the physical length of the former is about

half that of the latter. A directivity of 14.2 dB_i can be achieved by using a 19-segment coaxial–colinear antenna.

ACKNOWLEDGMENT

The author would like to thank the reviewers for their useful comments. He would also like to thank Dr. W.-J. Chiu, M.-P. Shih, L.-J. Yang, Dr. T.-T. Su, Dr. F.-H. Chen, Dr. K.-S. Huang, and their colleagues.

REFERENCES

- [1] Y. Wang and D. Fan, "Accurate global solutions of EM boundary-value problems for coaxial radiators," *IEEE Trans. Antennas Propagat.*, vol. 42, pp. 767–770, May 1994.
- [2] T.-D. Nhat and R. H. MacPhie, "The admittance of a monopole antenna fed through a ground plane by a coaxial line," *IEEE Trans. Antennas Propagat.*, vol. 39, pp. 1243–1247, Aug. 1991.
- [3] R. D. Nevels, "The annular aperture antenna with a hemispherical center conductor extension," *IEEE Trans. Antennas Propagat.*, vol. 35, pp. 41–45, Jan. 1987.
- [4] B. B. Balsley and W. L. Ecklund, "A portable coaxial collinear antenna," *IEEE Trans. Antennas Propagat.*, vol. AP-20, pp. 513–516, July 1972.
- [5] T. J. Judasz, W. L. Ecklund, and B. B. Balsley, "The coaxial collinear antenna: Current distribution from the cylindrical antenna equation," *IEEE Trans. Antennas Propagat.*, vol. AP-35, pp. 327–331, Mar. 1987.
- [6] T. J. Judasz and B. B. Balsley, "Improved theoretical and experimental models for the coaxial collinear antenna," *IEEE Trans. Antennas Propagat.*, vol. 37, pp. 289–296, Mar. 1989.
- [7] R. C. Hansen, "Evaluation of the Synder dipole," *IEEE Trans. Antennas Propagat.*, vol. AP-35, pp. 207–210, Feb. 1987.
- [8] S. Papatheodorou, J. R. Mautz, and R. F. Harrington, "The aperture admittance of a circumferential slot in a circular cylinder," *IEEE Trans. Antennas Propagat.*, vol. 40, pp. 240–244, Feb. 1992.
- [9] J.-F. Kiang, "Radiation properties of circumferential slots on a coaxial cable," *IEEE Trans. Microwave Theory Tech.*, vol. 45, pp. 102–107, Jan. 1997
- [10] L. C. Shen and J. A. Kong, *Applied Electromagnetism*, 3rd ed. Boston, MA: PWS, 1995.
- [11] R. F. Harrington, *Time-Harmonic Electromagnetic Fields*. New York: McGraw-Hill, 1993.
- [12] ———, *Field Computation by Moment Methods*. New York: IEEE Press, 1993.



Jean-Fu Kiang (M'89) was born in Taipei, Taiwan, R.O.C. on February 2, 1957. He received the B.S.E.E. and M.S.E.E. degrees from National Taiwan University, Taipei, Taiwan, R.O.C., and the Ph.D. degree from Massachusetts Institute of Technology, Cambridge, MA, in 1979, 1981, and 1989, respectively.

He has been with IBM Watson Research Center, Yorktown Heights, NY (1989–1990), Bellcore, Red Bank, NJ, (1990–1992), and Siemens, Danvers, MA (1992–1994). He is now with the Department of Electrical Engineering, National Chung-Hsing University, Taichung, Taiwan.